第62卷 第1期
2024年1月

古 脊 椎 动 物 学 报
VERTEBRATA PALASIATICA

pp. 47–68
figs. 1–6

DOI: 10.19615/j.cnki.2096-9899.230616

A skull of Early Pleistocene *Paracamelus gigas* (Artiodactyla, Mammalia) from Luotuo Hill in Dalian, Northeast China

DONG Wei[1] LIU Wen-Hui[2] BAI Wei-Peng[3] LIU Si-Zhao[4]
WANG Yuan[1] LIU Jin-Yuan[4] JIN Chang-Zhu[1]

(1 *Key Laboratory of Vertebrate Evolution and Human Origins of Chinese Academy of Sciences*, *Institute of Vertebrate Paleontology and Paleoanthropology*, *Chinese Academy of Sciences* Beijing 100044 dongwei@ivpp.ac.cn)
(2 *National Museum of China* Beijing 100006)
(3 *Institute of Nihewan Archaeology*, *College of History and Culture*, *Hebei Normal University* Shijiazhuang 050024)
(4 *Dalian Natural History Museum* Dalian 116024)

Abstract Originated in North America in the Middle Eocene, camelids were a successful group with very large diversity. But the camels emigrated to the Old World from North America, probably during the middle stage of the Middle Miocene, and did not radiate much as those in North America, represented by only two genera *Paracamelus* and *Camelus*. The former was considered as giving rise to the latter, but the detailed relationship of the Old World camelines was controversial. The new camel material unearthed from Layer 4 in the Jinyuan Cave at Luotuo Hill in Dalian, Liaodong peninsula in Northeast China, was described and referred to as *Paracamelus gigas*. Its dentition length is slightly longer than that of *Camelus knoblochi* but evidently larger than that of *C. ferus* and *C. dromedarius*. Based on the fossil records and morphometric evidences, *P. gigas* originated from a form similar to *P. alexejevi* in the Late Pliocene in the Old World, instead of from *Megatylopus gigas* of North America and then migrated into Asia as previously thought. The morphometric similarities between the Early Pleistocene Dalian specimens and those of the Middle and Late Pleistocene *C. knoblochi* indicate that *P. gigas* probably gave rise to *C. knoblochi* as formerly postulated and likely in the late Early Pleistocene by reduction or simplifying of P3 and P4, disappearance of p3 and shortening of dentition length. *P. gigas* inhabited in the forest steppe environment of Liaodong peninsula from 1.1 to 1.52 Ma based on paleomagnetic dating and pollen evidence.

Key words Dalian, Early Pleistocene, cave deposits, camel, *Paracamelus*, evolution

Citation Dong W, Liu W H, Bai W P et al., 2024. A skull of Early Pleistocene *Paracamelus gigas* (Artiodactyla, Mammalia) from Luotuo Hill in Dalian, Northeast China. Vertebrata PalAsiatica, 62(1): 47–68

1 Introduction

Based on the information provided by Mr. Guo Chengwan of the Angang clay mine of Fuzhouwan Sub-district, Professors Jin Changzhu of IVPP and Liu Jinyuan of Dalian Natural

中国科学院战略性先导科技专项(B类) (编号：XDB26030304)、大连金普新区管理委员会“大连普湾骆驼山第四纪脊椎动物化石综合研究”项目和中国科学院古生物化石发掘与修理专项资助。

收稿日期：2023-02-10

History Museum carried out a paleontological survey at Jinyuan Cave in a limestone quarry at the district in December of 2013. A locality with rich mammalian fossils was discovered from the cave deposits in the quarry (Liu et al., 2017a; Jin et al., 2021).

Jinyuan Cave fossil locality (39°24'3.69"N, 121°41'19.30"E, 70 m) is situated on the west side of Luotuo Hill (=Camel Hill). It is administratively affiliated to Fuzhouwan Sub-district of Jinpu New Area in Dalian of Liaoning Province, Northeast China.

The Luotuo Hill, an isolated hill along the direction of the northwest-southeast with a shape of a camel before quarrying and so named, locates west of Fuzhou Bay in Liaodong peninsula. Its strata are composed of Ordovician limestone of the Majiagou Formation (Liaoning Provincial Institute of Geological Exploration, 2013). Jinyuan Cave is a karstic cave developed in the limestone and filled with Plio-Pleistocene deposits with a visible thickness of more than 40 m and a basal width of 128 m.

The deposits can be divided into 6 layers (Liu et al., 2017a). Layers 1–3 yielded *Ursus deningeri*, *Ursus* cf. *U. etruscus*, *Canis* cf. *C. mosbachensis*, *Trogontherium cuvieri*, *Sus lydekkeri*, etc. (Jin et al., 2021), and the horizon is biochronologically equivalent to that of Locality 1 at the Peking Man site described by Li and Ji (1981), i.e. the Middle Pleistocene. Layers 4–6 yielded *Megantereon nihowanensis*, *Trogontherium cuvieri*, *Pachycrocuta brevirostris licenti*, *Mammuthus meridionalis*, *Leptobos brevicornis*, *Cervus* (*Sika*) *magnus*, *Axis shansius*, etc. (Jin et al., 2021), the horizon is biochronologically equivalent to that of Gongwangling Lantian Man site described by Hu and Qi (1978), i.e. the Early Pleistocene.

A large quantity of fossil specimens were collected from the deposits. The described taxa include *Pachycrocuta brevirostris* from Layers 3–5 (Liu et al., 2021), *Martes crassidens* from Layers 4–5 (Jiangzuo et al., 2021), *Episiphneus dalianensis* from the lowermost deposits (Qin et al., 2021), *Trogontherium cuvieri* from Layers 3–5 (Yang et al., 2021), *Hipparion* (*Proboscidipparion*) *sinense*, *H.* (*P.*) *pater*, *H.* (*Plesiohipparion*) *shanxiense* and *Hipparion* sp. from Layers 3–5 and the lowermost deposits (Sun et al., 2021a), *Equus qingyangensis* from Layer 3 (Sun et al., 2021b), *Axis shansius* (Bai et al., 2017), *Cervus* (*Sika*) *magnus* (Liu et al., 2017b) and *Eucladoceros boulei* from Layer 4 (Pan et al., 2020), and even birds from Layer 2 (Stidham et al., 2021). And interestingly, a broken skull and a mandibular fragment of camel fossils were uncovered from the cave deposits of the camel hill. Here we describe the camel specimens from Layer 4 of the locality. We followed the anatomic terminology for skull by Pacheco Torres et al. (1986) and that by König and Liebich (2009), and dental terminology by Dong (2004).

The described specimens are housed in the Dalian Natural History Museum. The compared extant specimens include the skulls of *Camelus ferus* (c/o.20, ov705, ov676), *C. dromedarius* (ov25) and *Lama glama* (ov251, ov1351) are housed in the Institute of Vertebrate Paleontology and Paleoanthropology, Chinese Academy of Sciences (IVPP).

2 Systematic paleontology

Mammalia Linnaeus, 1758
Artiodactyla Owen, 1848
Tylopoda Illiger, 1811
Camelidae Gray, 1821
Camelinae Zittel, 1893
Camelini Nordmann, 1850
***Paracamelus* Schlosser, 1903**
***Paracamelus gigas* Schlosser, 1903**

Revised diagnosis A large camel with a dentition length slightly longer than that of *Camelus knoblochi* but evidently larger than that of *C. ferus* and *C. dromedarius*. Skull narrow but long. Both upper and lower first premolars are present and caniniform. Both upper and lower third premolars are also present and little reduced. Metacarpus and metatarsus are long.

Material A broken skull with complete right and left dentitions (DLJ168001), a right mandibular fragment with a broken m2 and a complete m3 (DLJ1610-04). All specimens were unearthed from Layer 4 in the Jinyuan Cave at Luotuo Hill in Dalian described above and referred as Dalian specimens hereinafter.

Description The preserved skull DLJ168001 is broken but only slightly distorted. It is composed of a pair of most parts of nasals, a pair of nearly complete premaxillae with lateral incisors, a pair of nearly complete maxillae with canines and cheek teeth and large parts of palatines (Figs. 1–2). The nasals are long, narrow, nearly straight and roughly parallel to the palate, and they aligned side by side to form the roof of the nasal cavity. They arch upwards along sagittal plan that they can be seen clearly in lateral view. The anterior edge of the nasals is right above caniniform P1. The premaxillae are long, narrow and curved laterally and lie along the anterior borders of the maxillae, and they form the rostral edges of ventral and lateral walls of nasal cavity. Their alveolar processes point forward with the third incisors I3 emerging from the posterior side of the processes. The nasal processes of premaxillae contact directly with the anterior borders of processes of the nasals. A pair of fusiform palatine fissures lie between premaxillae and maxillae and they are separated from each other by 8–12 mm. The maxillae are massive, roughly trapezoid in lateral view. The right maxilla is better preserved than the left one. Their zygomatic processes and orbital faces (facies orbitalis) are broken off. Their rostral parts are tapering anteriorly in lateral view but swelling in dorsal and ventral views. Their cheek parts expand laterally in dorsal and ventral views, and infraorbital foramens are located about 30 mm above the base of the P4 with a diameter of about 8 mm in lateral views. The ventral horizontal laminae of the maxillae form the rostral and the major parts of the hard palate. A pair of palatine foramens are centrally located on each horizontal lamina of palatine processes of maxillae in ventral view, the right one is beside M1 and the left one between M1 and M2. The transverse palatine suture between maxillae and horizontal

laminae of palatines is arched in ventral view. The latter, i.e. the caudal and minor parts of the hard palate are archivolt in ventral view. Their anterior borders start from the intersection of the connecting line between the centers of right and left M2 and the palatine sagittal suture, and the lateral borders run along the maxillary alveolar bases of M2–3. Each caudal nasal spine is located in the caudal center of each horizontal lamina with two notches, i.e. lateral palatal notches, on its both sides. The caudal parts of the caudal spines of the palatines are not preserved. The choanae, or posterior nares, are located just behind the caudal central border of the palatines and within right and left caudal spines. The palatine fossae are very developed and their anterior borders, or lateral palatal notches, reach the line between right and left posterior lobes of M3. The medial and lateral palatal notches are all vaulted.

The preserved upper dentitions are complete, including I3, C, P1 and P3–M3 and in accordance with the dental formula 1-1-3-3 as most fossil camelids. The dentitions are fully erupted, worn in certain degree, and that indicates a middle to old age. The P2 is absent. The measurements of the upper teeth are listed in Table 1. There are significant diastemas between I3 and C, between C and P1, as well as between P1 and P3. That between I3 and C is about two thirds of that between C and P1, and about one third of that between P1 and P3.

The I3 is caniniform. The tip of the left I3 is broken off, but the right one is complete. The crown is hypsodont, or vertically long, conical and mildly bend forward. The crown cross

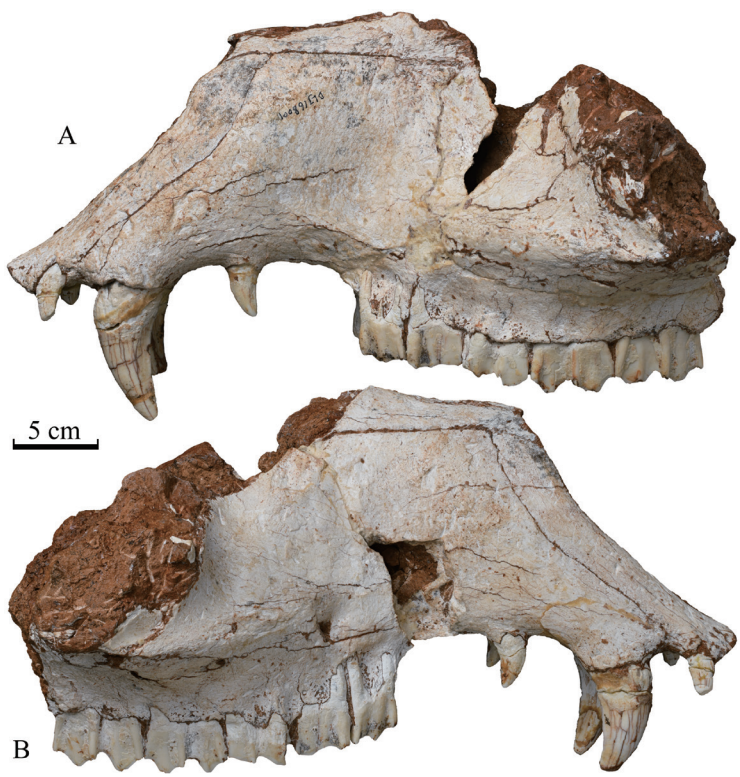

Fig. 1 The broken skull (DLJ168001) of *Paracamelus gigas* from Jinyuan Cave, Dalian
A. left lateral view; B. right lateral view

sections are roughly fusiform and their mesial edges are relatively obtuse while the distal ones comparatively sharp.

The C is robust and horn-like, indicating its male character. The mesiodistal and linguo-vestibular diameters of the crown are nearly triple those of the I3, and the basal-tip height of the crown, or vertical length, nearly quadruple size of the I3. The cross sections of the crown are between oval and fusiform with the mesial edges moderately obtuse while the distal ones somewhat keen.

The P1 is also caniniform and located in the lip zone instead of in the cheek zone as in typical ruminants. It is morphologically very similar to I3, but its size is moderately larger.

The upper cheek teeth, i.e. those from the third premolar to the third molar, are typically selenodont and mesohypsodont (Figs. 1–2).

The P3 is developed as in typical *Paracamelus*. It is composed of one lobe with two main cusps, i.e. protocone and paracone, and the buccal cusp is larger than the lingual one. The occlusal surface of the crown is not typically crescent. The protocone is well developed, but both preprotocrista and postprotocrista are relatively thin and contracted buccally. The paracone is also well developed, as well as parastyle and metastyle. The preparacrista and postparacrista are also thin. The trigon basin, or prefossette, is mesiodistally elongated and narrow. No cingulum is present on mesial, lingual and distal sides of the crown base, but a weak crest is present on the buccal side of the crown base, as a vestige of ectocingulum or buccal cingulum.

The P4 is also composed of one lobe with two main cusps, but its size is much larger than that of P3 and the occlusal surface of the cusps are more crescent than in P3. The protocone is well developed, both preprotocrista and postprotocrista are worn and their bases fused with protocone to form a lingual crescent loph. The paracone is also well developed, and both preparacrista and postparacrista are worn and fused with paracone to form a buccal crescent loph. The parastyle and metastyle are also developed as in P3. The trigon basin is mesiodistally elongated, narrow and curved lingually. No cingulum is present on mesial, lingual and distal sides of the crown base, entoflexus either. As in P3, a weak crest is present on the buccal side of the crown base. Medial crista is present on the buccal side of postprotocrista, but not well developed.

The M1 is composed of two lobes, or four selenodont main cusps, with the protocone and metaconule on the lingual side and paracone and metacone on the buccal. The width of the main cusps is larger than the length of those. The first lobe is quite worn that the trigon basin, or prefossette, is invisible. But the second one is less worn and the talonid basin, or postfossette, is still visible.

The M2 is also composed of two lobes with four main cusps as in M1. But the length of the main cusps is larger than the width of those. The tooth is less worn than M1 that the occlusal structure is much more visible than that in M1. The anterior and posterior cristae of the main cusps are completely fused with the cusps to form selenodont lophs. Besides the

selenodont main cusps, the trigonid basin and talonid basin, or prefossette and postfossette, are also selenodont. The parastyle, mesostyle and metastyle are developed, but parastyle and mesostyle are more developed. The pillar of parastyle inclines mesially from the base to the occlusal surface while that of metastyle distally that the pillars form an angle about 20°. Ectocingulum or buccal cingulum remains as a vestige.

The M3 is similar to M2, but the crown is less worn, its occlusal dimensions are longer and narrower.

The lower dentition is represented by a right mandibular fragment with a broken m2 and a complete m3 (DLJ1610-04). The worn crown indicates its old age (Fig. 3). The measurements of the lower teeth are listed in Table 2.

The preserved m2 is composed of a largely broken entoconid and a nearly complete hypoconid. The protoconid and metaconid are completely lost. The preserved part of

Table 1 Measurements of upper teeth of Dalian specimen and comparison (mm)

	Paracamelus gigas					*Camelus knoblochi*			*C. ferus*	*C. dromedarius*
	DLJ168001		Honan[1)]	Mianchi[2)]	Nihewan[3)]	Luchka[4)]	Razdorskaya[4)]	Sengiley[4)]	c/o.20.705.676	ov25
	left	right								
I3 L	14.42	16.06		12.8		20	21*	20	6.1-6.9	(9.5)
I3 W	10.27	11.97		9.1		15	17*	16	4.3-6.9	(7.2)
I3 H	19.37	20.6							9.9-18.7	
C L	39.63	40.18		16.4	20†	40*	22.0; 23.1	34; 37	11.9-12.1	12.4-12.7
C W	28.32	24.48		12.2	14†	29*			7.4-9.2	8.7-8.9
C H	80.05	56.22							17.6-29.3	
P1 L	17.57	19.16				22*		24; 23.2	9.1-9.5	8.7-8.9
P1 W	14.11	14.23				18*		19; 17	7.2-7.4	6.3-6.5
P1 H	31.18	33.16							22.1-22.8	17.1-17.9
P3 L	28.72	29.51		(28)	31	26	18; 18.7	28; 27	17.3-18.2	18.7-20.1
P3 W	21.52	23.14		(20)	21	25.5	17; 17	20; 22	13.8-15.1	12.7-13.5
P3 H	24.91	25.71							16.2-19.2	27.1-29.2
P4 L	32.67	33.35		30	29	27; 28	22.4; 24	29.5; 31	19.1-22.9	23.6-24.3
P4 W	30.19	39.63		29.6	28	29.4; 29	27.1; 28	29; 29.3	18.4-25.9	22.3-23.3
P4 H	27.82	29.15							18.7-23.3	23.9-25.7
M1 L	37.46	37.32	47§	(36)	38	33.3; 31	34.3; 34.4	32.8; 33.8	25.8-32.1	26.9-30.6
M1 W	41.84	36.15	38§	38.5	37	34; 33	33; 34.1	34.2; 34.2	30.1-33.2	29.1-30.7
M1 H	24.82	24.97	25§						19.4-24.9	11.7-21.1
M2 L	48.48	47.36	50	(46)	45.5#	51	42; 41.6	54.3; 53	37.2-45.2	39.8-40.2
M2 W	39.34	38.35	41	42.4	35.0#	38	36.6; 37.9	37.3; 35.3	31.1-35.8	28.9-31.1
M2 H	30.75	31.87	36						19.3-28.9	24.3-24.4
M3 L	51.98	52.23		55	43.0#	59	52; 52.7	61.4; 61.3	39.9-46.2	42.2-44.7
M3 W	35.99	35.74		43.3	34.5#	35	36.1; 36.8	35; 25	24.3-32.3	27.1-31.6
M3 H	33.79	35.08							20.1-22.5	27.8-30.1
Di I3-C	20.51	23.28		18		21.0	14*		12.1-16.8	10.9
Di C-P1	33.4	37.61			72†		16*		30.1-41.7	35.4-35.9
Di P1-3	61.62	59.79			>60	51.0; 49.0	49*		24.1-43.8	43.9-47.8
P3-4 L	61.59	64.63		(58)			38.5; 39.2		37.2-39.8	35.1-39.1
M1-3 L	136.35	136.85		(131)		140	123; 124	144; 142.3	104.1-112.4	111.2-115.9
P3-M3 L	199.6	203.5		(186)		184			135.7-145.3	141.1-143.7

Notes: the values in brackets are estimated ones. L. length; W. width; H. height; Di. diastema.

Data source: 1) Schlosser, 1903; 2) Zdansky, 1926; 3) Teilhard de Chardin and Trassaert, 1937; 4) Titov, 2008; † from Haiyan in Yushe Basin (Liu et al., 2023); * from Salawusu (=Sjara-osso-gol) (Boule et al., 1928); # *Paracamelus* sp. from Yegou (Liu et al., 2022); § probably from Tianjin, Made et al. (2002) considered it might represent an M2.

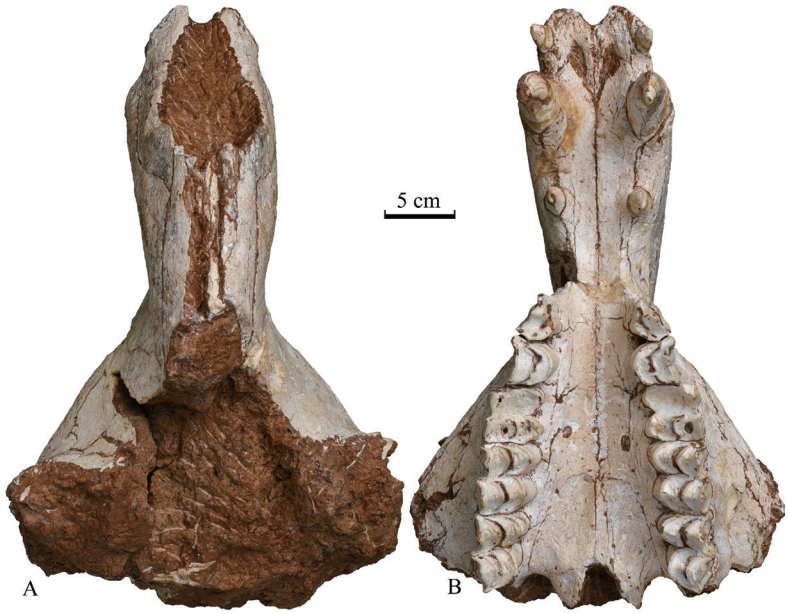

Fig. 2 Broken skull (DLJ168001) of *Paracamelus gigas* from Jinyuan Cave, Dalian
A. dorsal view; B. ventral view

entoconid is its buccal enamel wall, arched buccally and mesohypsodont. The hypoconid is fused with prehypocristid and posthypocristid to form a selenodont cuspid. The talonid basin, or postfossette, is long, thin and crescent. The accessary elements such as ectostylid, ectocingulid and postcingulid are all absent.

The m3 is composed of three lobes. Both first and second lobes are evidently composed of two main selenodont cuspids respectively. The third lobe should be composed of two minor cuspids but fused together based on its width. The protoconid and hypoconid are thicker than metaconid and entoconid. The preprotocristid is thinner and longer than postprotocristid, and the prehypocristid is also thinner and longer than posthypocristid. The premetacristid and postmetacristid are still distinct from metaconid, the latter is thick and cylinder-like. The preentocristid and postentocristid are not distinct from entoconid and the occlusal view is somewhat fusiform. The parastylid and metastylid are moderate, while entostylid is very weak. Both trigonid and talonid basins are long, thin and crescent. Both hypoconulid and entoconulid are

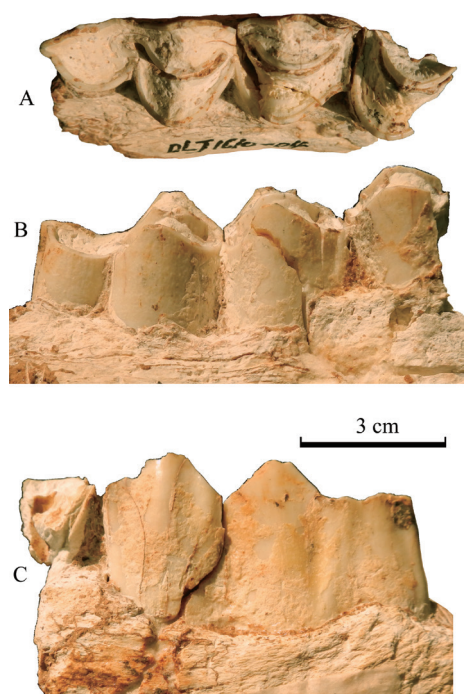

Fig. 3 The right mandibular fragment with broken m2 and complete m3 (DLJ1610-04) of *Paracamelus gigas* from Jinyuan Cave, Dalian

relatively small, and the former is evidently larger than the latter. The hypotalonid basin is present but nearly invisible due to worn state of the last lobe.

Table 2 Measurements of lower teeth of Dalian specimen and comparison (mm)

Specimens	*Paracamelus gigas*			*Camelus knoblochi*			*C. ferus*	*C. dromedarius*
	DLJ1610-04	Yushe[1)]	Kossom Bougoudi[2)]	Luchka[3)]	Sengiley[3)]	Salawusu[4)]	c/o.20,705,676	ov25
m2 L		37–40	39.7	43	49.2		34.1–42.3	39.6–40.4
m2 W	(28)	23–26	23.7	31.4	28.4		21.8–26.1	19.1–20.2
m2 H	26.28						15.2–23.3	27.7–28.3
m3 L	62.97	54–58	54.4	73	72	65	54.1–57.3	52.1–56.3
m3 W	28.52	22–25	21.5	29.4	25.5		19.5–24.5	23.8
m3 H	26.27						18.9–20.4	26.1

Note: the value in brackets is estimated one. L. length; W. width; H. height.

Data source: 1) Teilhard de Chardin and Trassaert, 1937 and these mandibular fragments from the Yushe Basin were considered by Liu et al. (2023) as three different species of *Paracamelus* including *P. alexejevi*; 2) Likius et al., 2003; 3) Titov, 2008; 4) Boule et al., 1928 (Salawusu=Sjara-osso-gol).

Comparison Compared with *Paracamelus gigas* defined by Schlosser (1903) and probably bought from Tianjin and Henan, the general morphology between his specimens and Dalian ones are similar. The observable differences are that the paracone and mesostyle in upper molar from Tianjin are slightly bigger; the trigon and talon basins, or anterior and posterior fossettes, are wider; the basal "crest" on buccal side of cheek teeth is present in Dalian specimen but weaker than in Tianjin one. The dimensions of Tianjin specimen, a presumed M1, are larger than those of the M1 of Dalian specimen but slightly smaller than those of the M2. And those of Henan specimen, a presumed M2, are slightly larger than those of the M2 of Dalian specimen (Table 1).

Compared with *P. gigas* from Mianchi (Zdansky, 1926), *C. knoblochi* from Razdorskaya (Titov, 2008), extant *Camelus ferus* (c/o705) and *C. dromedarius* (ov25), the morphology of the preserved Dalian skull (DLJ168001) is similar to that of both extant *Camelus ferus* and *C. dromedarius*, as well as *C. knoblochi* from Razdorskaya. But the premaxillae and nasals of Dalian specimen are relatively wider, the nasals are moderately arched upwards instead of relatively flat. The naso-premaxilla process of maxilla is protruding forwards in *C. ferus* and *C. dromedarius*, but without protruding in Dalian specimen. The right and left lateral borders of the nasals are nearly straight in Dalian specimen but laterally expanded as fusiform in dorsal view in *C. ferus* and *C. dromedarius*. In ventral view (Fig. 4), the hard palate of Dalian specimen is more similar to that of *C. ferus* and *C. dromedarius* than to that of *C. knoblochi*. The palatine foramen is in the palatine process of the maxilla and corresponding to the metastyle of M1 in Dalian specimen and to the mesostyle of M1 in *C. dromedarius*, on the suture between the palatine process of maxilla and palatine bone and parallel to the protocone of M2 in *C. ferus*, on the suture and parallel to the parastyle of M3 in *C. knoblochi* and invisible in *P. gigas* from Mianchi. The anterior part of the suture between maxilla and the palate bone is parallel to the mesostyle of M2 in Dalian specimen and *C. dromedarius*, but parallel to the paracone of M3 in *C. ferus*, and parallel to the parastyle of M3 in *C. knoblochi*, invisible in *P. gigas*. The medial palatal notch, i.e. the anterior edge of choana, is parallel to

the mesostyle of M3 in Dalian specimen and *C. dromedarius*, but parallel to the mesostyle of M2 in *C. ferus*, and behind M3 in *C. knoblochi* and *P. gigas*. The lateral palatal notch, i.e. the anterior edge of palatal fossa, is parallel to the metaconule of M3 in Dalian specimen and *C. dromedarius*, parallel to the protocone of M3 in *C. ferus*, and about one lobe's distance behind M3 in *P. gigas* and *C. knoblochi*.

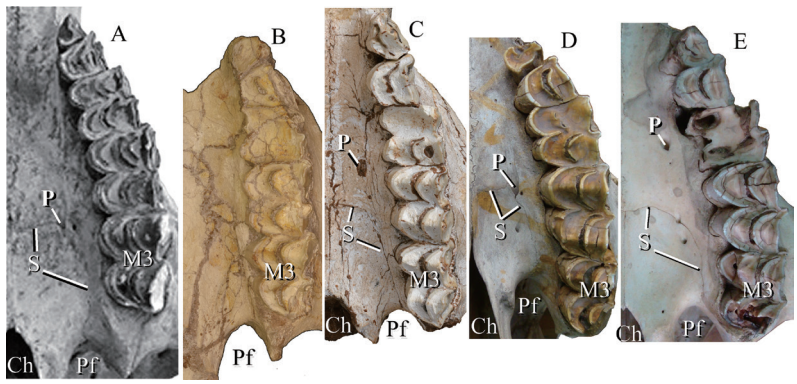

Fig. 4 Palatal comparison between Dalian specimen and related camels (not to scale)
A. *Camelus knoblochi* (Titov, 2008); B. *Paracamelus gigas* (Zdansky, 1926); C. *P. gigas* (DLJ168001); D. *C. ferus* (c/o705); E. *C. dromedarius* (ov25)
Abbreviations: Ch. choana; M3. upper third molar; P. palatine foramen; Pf. palatine fossa; S. suture between palate and maxilla

Compared with the other camelines, the I3 of Dalian specimen are evidently larger than those of *C. ferus* and *P. gigas* from other localities, but slightly smaller than those of *C. knoblochi*. The canines of Dalian specimen are much larger than those of *C. ferus*, *C. dromedarius* and *C. knoblochi*, as well as *P. gigas* from other localities (Table 1; Figs. 5–6). The caniniform P1 of Dalian specimen is slightly smaller than that of *C. knoblochi*, but larger than that of other camelids. The diastema between I3 and C of Dalian specimen is larger than that of *C. knoblochi*, *C. ferus* and *C. dromedarius*. The diastema between C and P1 of Dalian specimen is much smaller than that of *P. gigas* from Haiyan (Licent's Loc. 6) in Yushe Basin, clearly larger than that of *C. knoblochi*, but similar to that of *C. ferus* and *C. dromedarius* (Table 1). The diastema between P1 and P3 of Dalian specimen is slightly larger than that of *C. knoblochi*, but evidently larger than that of *C. ferus* and *C. dromedarius* (Table 1). In functional permanent cheek dentitions (Fig. 4), i.e. P3–M3, the morphology of Dalian specimen is generally similar to that of *P. gigas* from Mianchi (Zdansky, 1926), extant *C. ferus* and *C. dromedarius*, as well as the Pleistocene *C. knoblochi* from Russia (Titov, 2008). For example, the occlusal surface of the P3 is not typically crescent, no cingulum is present on any side of the crown base; the P4 is also composed of one lobe with two simply-built crescent main cusps; the M1–3 are composed of two lobes with four simply-built crescent main cusps without accessary elements. Nevertheless, the occlusal surface of P3 is about two thirds of that of P4 in Dalian specimen, about a half in *P. gigas* from Mianchi, and around one third in *C. knoblochi*, *C. ferus* and *C. dromedarius*; the P3 of Dalian specimen is much larger than that of *C. ferus*, *C.*

dromedarius and *C. knoblochi*, but similar to that of the *P. gigas* from Mianchi and Nihewan (Table 1, Figs. 4–6) and that clearly indicates its generic attribution of *Paracamelus* (Zdansky, 1926; Teilhard de Chardin and Trassaert, 1937; Wang and Wu, 1979). The P4 of Dalian specimen is clearly larger than other camelids; in addition, both lingual and buccal walls of P4 are more undulate than those of other camelids, a few folds are present on the buccal wall of paracone in Dalian specimen and *P. gigas* from Mianchi (Fig. 4). The main cusps of molars, both lingual and buccal ones, are arched lingually. But the direction of the curve deflects in certain degree in Dalian specimen and *P. gigas* from Mianchi, but without deflection in *C. ferus*, *C. dromedarius* and *C. knoblochi* (Fig. 4). The dimensions of M1 in Dalian specimen are similar to those in the *P. gigas*, slightly larger than those of *C. knoblochi*, evidently larger than those of *C. ferus* and *C. dromedarius*. And those of M2 in Dalian specimen are similar to those in *P. gigas* and *C. knoblochi*, but clearly larger than those in *C. ferus* and *C. dromedarius*. While those of M3 in Dalian specimen are smaller than those in the *P. gigas*, similar to those in *C. knoblochi*, and larger than those in *C. ferus* and *C. dromedarius*. Compared with the *Paracamelus* sp. from the Upper Neogene at Lingtai (Zhang et al., 1999), Dalian specimen is much larger, the P4 is more complicated. Compared with the *Paracamelus* sp. from the Upper Pliocene dark brownish grey silty clay at Yegou in Nihewan Basin (Liu et al., 2022), the M2 of Dalian specimen is slightly larger, but the M3 is evidently larger (Table 1), and the posterior lobe of the M3 is not significantly contracted as in Yegou specimen. As to the dentition length, that from I3 to M3, Dalian specimen is slightly longer than that of *C. knoblochi* but evidently longer than that of *C. ferus* and *C. dromedarius* (Table 1).

The preserved m2 of Dalian specimen, an incomplete posterior lobe of m2 and characterized by its rounded hypoconid, is morphologically comparable with that of extant *C. ferus* and *C. dromedarius*, but metrically larger (Table 2); while it is slightly larger than that of *P. gigas* from Yushe and Kossom Bougoudi but slightly smaller than that of *C. knoblochi* (Table 2) and the hypoconid of that of *P. gigas* from Kossom Bougoudi is slightly pointed buccally (Likius et al., 2003). The well preserved m3 of Dalian specimen is morphologically similar to that of *P. gigas* from Mianchi and Yushe, particularly the specimen No. 12987 (Teilhard de Chardin and Trassaert, 1937), although the specimen was considered by Liu et al. (2023) as a new species of *Paracamelus*, but its dimensions are evidently larger (Table 2). It is morphologically similar to that of *C. knoblochi* from Salawusu (Boule et al., 1928), but its dimensions are smaller. It is also morphologically similar to that of *C. dromedarius*, but the trigonid and talonid basins are narrower in Dalian specimen than in *C. dromedarius*. It differs from that of *C. ferus* by the third lobe, which is semicircular in the former and elongated triangular in the latter. It is worthwhile to mention that *P. gigas* was also recovered from Kossom Bougoudi, northern Chad. The right mandibular fragment with p3–m3 (KB3.97.316) is also comparable with Dalian specimen, e.g. rounded buccal main cuspids, narrow trigonid and talonid basins, but Dalian specimen is slightly larger (Table 2). The Ratio diagrams of dentition lengths and widths of different camels, plotted against Dalian specimens (Figs. 5–6), show that the dimensions of upper incisor and cheek teeth

of Dalian specimen are the closest to those of *P. gigas* from other localities, although those of upper canine of Dalian specimen are evidently larger. The dimensions of P3 and the length of P3–4 of *P. gigas* of both Dalian specimen and those from other localities are larger than those of Russian *C. knoblochi*, extant *C. ferus* and *C. dromedarius*. It strengthens the diagnoses of *Paracamelus* that its P3 is not contracted as *Camelus*. The dimensions of I3, P1 and M2–3 of *C. knoblochi* are larger than those of *P. gigas*, but the dentition length of Dalian specimen is longer than that of *C. knoblochi*. The extant *C. ferus* and *C. dromedarius* are smaller than fossil *C. knoblochi* and *P. gigas*. As a geographically remote extant relative, South American *Lama glama* is significantly smaller than its Asian relatives, both fossil and extant ones.

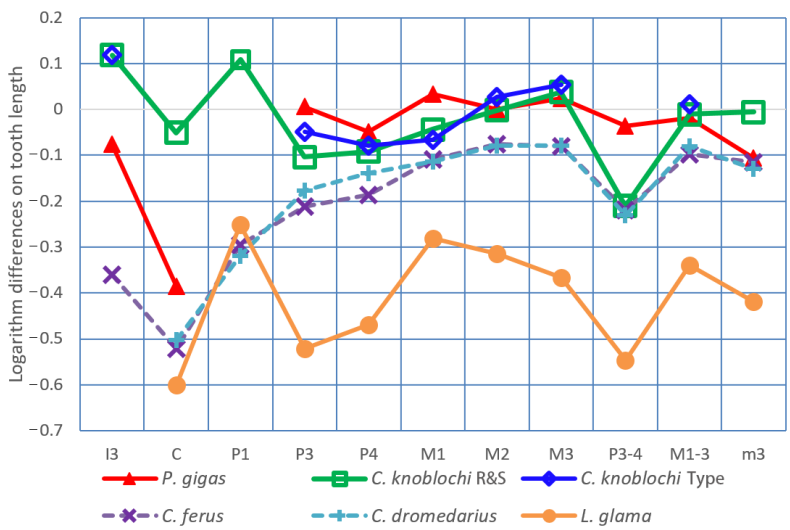

Fig. 5 Ratio diagram of dentition lengths of different camels, plotted against Dalian specimens (reference 0)
Data source: as in Tables 1 & 2; R&S. Razdorskaya and Sengiley

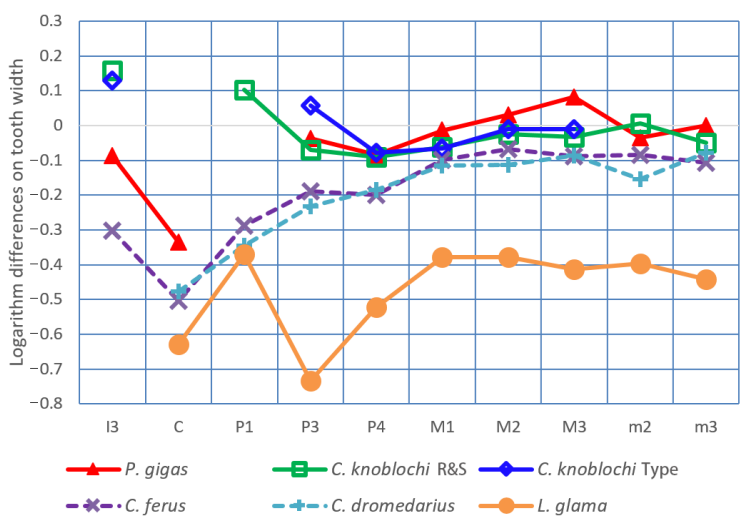

Fig. 6 Ratio diagram of dentition widths of different camels, plotted against Dalian specimens (reference 0)
Data source: as in Tables 1 & 2; R&S. Razdorskaya and Sengiley

3 Discussion

3.1 Discovery and distribution of *Paracamelus gigas*

The first fossil camel from China was reported by Schlosser (1903) and was named as *Paracamelus gigas* based on two upper molars collected from traditional Chinese medicine stores. A presumed M1 was probably from Tianjin and a presumed M2 probably from Henan. But only the former was figured by Schlosser (1903) and it was regarded as (lecto)type by Made and Morales (1999). It was considered as sharing a common ancestor with *Camelus sivalensis* (Schlosser, 1903). Since its provenance and horizon were uncertain, the presumed M1 differed from those of *Camelus* in that both the mesostyle and the buccal pillar of the paracone are distinctly broader, especially near the base, the central anterior valley was wider, and the buccal crescents had a less regular thickness, Geraads et al. (2021) even questioned its taxonomic status as a camelid. Their doubts seem reasonable, especially that the bases of mesostyle and paracone of Tianjin specimen are larger, i.e. somewhat phyllophagous pattern, but it would be normal for earlier camelids adapted for forest-steppe environment. The parastyle and buccal pillar of paracone of P3, the parastyle and mesostyle of M3 in Dalian specimen are also broader towards the base (Fig. 1), but less evident than Tianjin specimen. As to wider central valley and less thick crescents, the Tianjin specimen was figured in a view not fully parallel to the occlusal surface of the molar, but with an oblique angle that resulted the widening of the valley due to the different occlusal surface levels and orientations of buccal and lingual main cusps and narrowing the crescents as the case of the M3 in Fig. 4D illustrated above.

Zdansky (1926) described an incomplete skeleton of camel from the red clay at Yangshao Village of Mianchi County in Henan Province. He regarded the material, larger than extant ones, the closest to that of *P. gigas* defined by Schlosser (1903), and then to *Megatylopus gigas* defined by Matthew and Cook (1909) from North America, but different from the fossil camels from Europe and the Siwaliks (Zdansky, 1926). He admitted the validity of *Paracamelus* named by Schlosser based on two isolated molars only and justified the validity by four characters observed from Mianchi specimens. The material described by Zdansky increased a lot the morphological data of *P. gigas* and the specimens from Mianchi were served as reference of Schlosser's *P. gigas* for comparison by later researchers (e.g. Teilhard de Chardin and Piveteau, 1930; Young, 1932; Teilhard de Chardin and Trassaert, 1937; Tang, 1980; Likius et al., 2003).

Teilhard de Chardin and Piveteau (1930) reported a calcaneus and a distal part of radius from Xiashagou in Nihewan Basin and considered them as identical to those from Mianchi and included them into *P. gigas*. They suggested it as the direct ancestor of *C. knoblochi* from Salawusu described by Boule et al. (1928). But they questioned Zdansky's indication that *P. gigas* differed from extant camels by the absence of both upper and lower caniniform first premolars.

An almost complete right hind foot of a giant camel from Locality 1 of Zhoukoudian Site, differed from the corresponding parts of *C. bactrianus* by an extraordinary larger size, was described and considered by Young (1932) as the same as that of Zdansky's *P. gigas*. He noted that the stratigraphic provenance of Zdansky's *P. gigas* was not certain if it was equivalent to that of Nihewan or Loc. 1 of Zhoukoudian. But he thought the genus *Paracamelus* could be retained provisionally, and its confirmation needed better preserved premolar series, e.g. the proved presence of lower third premolar. The Zhoukoudian material was considered from Layer 11 of Loc. 1 (Li and Ji, 1981), which was dated as 462 ka by ESR/U (Zhao et al., 1985) and as 770±80 ka by $^{26}Al/^{10}Be$ (Shen et al., 2009), i.e. within the Middle Pleistocene, and it was its last appearance in China. Nevertheless, Liu et al. (in preparation) doubted the taxonomic status of Zhoukoudian specimens as *P. gigas*.

Later on, Teilhard de Chardin and Trassaert (1937) included some upper and lower jaw specimens and limb bones from the Yushe Basin into *P. gigas*, together with a few maxillary and mandibular fragments as well as some limb bones from Nihewan collected later than those described by Teilhard de Chardin and Piveteau (1930). They revised the definition of *P. gigas* and confirmed the presence of both upper and lower caniniform first premolars as well as both upper and lower third premolars in *P. gigas*, and the generic status of *Paracamelus* was thus settled. They regarded, in addition, *P. gigas* as in the direct line leading to the living *C. bactrianus.* Although Teilhard de Chardin and Trassaert (1937) indicated that their specimens were from Zone III, i.e. equivalent to the Plio-Pleistocene, but the fossil localities include not only Haiyan, but also Gaozhuang, Yinjiao, Wuxiang, etc. (Teilhard de Chardin and Trassaert, 1937) with Gaozhuangian or probably earlier faunas (Liu et al., 2023). That means the deposits yielding *P. gigas* in Yushe Basin might range at least from the Pliocene (Gaozhuangian ≈ Ruscinian) to the Early Pleistocene based on the stratigraphic correlation by Qiu et al. (1987; 2013) and that was the earliest appearance of *P. gigas* in China.

Two left isolated lower first and second molars were collected from the Early Pleistocene deposits alongside of the Yellow River at Linyi in southern Shanxi Province. The teeth are larger than those from Yushe Basin and were identified as *Paracamelus* sp. (Tang et al., 1983). It might be a variety of *P. gigas*.

P. gigas was no longer reported from China until the appearance of Dalian specimens. While it was noted by Morales (1984) that it was found in Afghanistan and Iran. And it was also found in the Koshkurgan (=Vyatka) Faunal Complex of the Middle Pleistocene in Kazakhstan (Howell et al., 1969; Shpansky et al., 2016), and even from the fossiliferous area with an age around the Mio-Pliocene boundary (ca 5 Ma) at Kossom Bougoudi in Nord Chad, represented by a fragment of mandible and two complete metapodials (Likius et al., 2003). The horizon is chronologically similar to that of the lower boundary of Gaozhuangian in Yushe Basin, the earliest appearance of *P. gigas* in East Asia up to that time. A *Paracamelus* cf. *P. gigas* was reported from Khapry deposits exposed along the north coast of the Taganrog gulf of the Sea of Azov and the left bank of the lower current of the Don River (Titov, 2003), as well

as from Podpusk-Lebyazhie Complex associated with MN17 Mammalian Zones in western Siberia (Shpansky et al., 2016). The geographic distribution of *P. gigas* seemed therefore quite wide, not only in Asia, but also in Africa. And the chronological distribution of *P. gigas* seemed ranging from the Latest Miocene to the Middle Pleistocene.

Nevertheless, Liu et al. (2023) indicated in their recent review on 17 specimens of *Paracamelus* from 12 localities in the Yushe Basin that only four specimens from Upper Mazegou Formation and Haiyan Formation could be included into *P. gigas*, the others could be included into four other species of *Paracamelus*. The Paleomagnetic age of *P. gigas* in Yushe Basin was estimated within 3–2.15 Ma, the earliest record of *P. gigas* is therefore not earlier than 3 Ma. Consequently, the other specimens of *P. gigas* discovered in Europe and Africa needed a corresponding revision.

3.2 Relatives of *P. gigas*

Zhang et al. (1999) reported a maxillary fragment with right and left P3–M3 and some limb bones of a camel from a fossiliferous horizon in the Upper Neogene red clay with a paleomagnetic age of 3.4–3.5 Ma at Renjiagou, Lingtai County, Gansu Province. The specimens were included into *Paracamelus* sp. and appeared smaller and more primitive than those of *P. gigas* and it was considered by Liu et al. (2023) as *P. alexejevi.*

A right isolated M2 and a right isolated M3, as well as a distal portion of the left humerus and a manual 4th proximal phalanx from the Upper Pliocene dark brownish grey silty clay at Yegou in Nihewan Basin were assigned to *Paracamelus* sp. (Liu et al., 2022). The dental morphology and dimensions of Yegou specimens are between those of Dalian specimen and Renjiagou ones. The phalanx from Yegou is distinctly larger than that of *P. gigas* from Loc. 1 of Zhoukoudian described by Young (1932) and that from Mianchi described by Zdansky (1926), and even larger than that of extant camels (Liu et al., 2022). The Yegou specimens represent probably a new variety of *Paracamelus*. The genus might therefore be represented by five to six species in China.

Other relatives of *P. gigas*, or other species of *Paracamelus*, according to Made et al. (2002), included *P. khersonensis* (from upper Sarmatian of Kherson in Ukraine), *P. alutensis* (from the Pleistocene in Slatina area of Rumania), *P. bessarabiensis* (from the Late Pliocene in Bessarabia), *P. kuljenensis* (= *kujalnensis*), *P. praebactrianus*, *P. alexejevi* (from the Middle Pliocene of Odessa in Ukraine) and *P. aguirrei* (from the latest Miocene of Venta del Moro in Spain). Among these species, Kostopoulos and Sen (1999) and Titov (2003) agreed the view that *P. kujalnensis* from "kujalnik" deposits of the Black Sea region was the junior synonym of *P. alutensis.* But Titov (2003) agreed the presence of two other species: *P. longipes* from the Middle Pliocene of Kazakhstan and *P. trofimovi* from the Late Pliocene of Kuruksay, Tajikistan. While Geraads et al. (2021) regarded *P. longipes* from Kazakhstan as *P. gigas*. On the other hand, Logvynenko (2001) named a new species *P. minor* from Odessa, the northern Black Sea area in Ukraine and dated to the Middle Pliocene (late Ruscinian). He regarded it as a sister species of *P. alexejevi* from the same site and horizon, and it could give rise to

P. alutensis. A third *Paracamelus* from Odessa in Ukraine, *Paracamelus* cf. *P. aguirrei*, was reported from the Pontian deposits by Titov and Logvynenko (2006). It was also found from the Late Miocene deposits in Buldynka, and Yabloniya near Odessa in Ukraine, Eupatoria in Crimea, as well as from Sinyavskaya and Novocherkassk in Russia (Titov and Logvynenko, 2006). Nevertheless, *P. minor* from Odessa was considered as junior synonym of *P. alutensis*, as well as *P. kujalnensis* (Geraads et al., 2021).

A *Paracamelus* sp. was reported from Verduno in northern Italy and dated about 5 Ma (Colombero et al., 2017). *Paracamelus* also occurred in Afghanistan, as well as at Lake Ichkeul in Tunisia which was usually considered to be a "lower Villafranchian" (and thus Lower Pleistocene or Upper Pliocene) site (Pickford et al., 1995).

While Liu et al. (2023) indicated that *Paracamelus* included 12 taxonomically valid species, i.e. *P. gigas*, *P. sibiricus*, *P. alutensis*, *P. khersonensis*, *P. bessarabiensis*, *P. praebactrianus*, *P. alexejevi*; *P. longipes*, *P. aguirrei*, *P. trofimovi*, *P. minor* and a new species named by them.

Although widely cited species of *Paracamelus* include *P. gigas*, *P. aguirrei*, *P. alutensis* and *P. alexejevi* only, the diversity of the genus is nonetheless quite large. Its geographic range is mostly within Eurasia and North Africa, and its chronological range is mostly within the Late Neogene and Pleistocene. It is worthwhile to note that a large camel from the Late Pleistocene of Yukon of Canada was identified as Camelini cf. *Paracamelus gigas* (Harington, 2011; Rybczynski et al., 2013; Zazula et al., 2016). The material is very limited and the identification remains to be confirmed with more detailed material.

3.3 Origin of *Paracamelus* and evolution of *P. gigas*

Originated in the Middle Eocene, camelids were a highly successful group in North America, as Honey et al. (1998) summarized, and the radiation of Camelinae in North America began in the late Hemingfordian and early Barstovian (late Early to early Middle Miocene). The earliest record of *Paracamelus* in China was found in the Yushe Basin, at the beginning of Gaozhuangian (~5 Ma), between the Miocene and Pliocene (Qiu et al., 2013). While Vangengeim and Tesakov (2013) indicated that the most remarkable event in the early Pontian (MN12) near Odessa and Eupatoria, and Rostov-on-Don was the first occurrence of the genus *Paracamelus* dated from 7.5 to 7.1 Ma, and *Paracamelus* migrated to southern East Europe in the middle Turolian (MN12). It is therefore the earliest record of *Paracamelus* as well as the earliest record of camelines in the Old World. Vangengeim and Tesakov (2013) indicated further *Paracamelus* had a short-term westward dispersal only in the Messinian (MN13), but they did not specify which species of *Paracamelus* they discussed. Nevertheless, according to Titov and Logvynenko (2006), it was *Paracamelus* cf. *P. aguirrei*, a medium sized *Paracamelus*, distributed in Odessa, Eupatoria and Rostov-on-Don. Evidently, the earliest record of the Old World camelines is much later than that of North America and it is widely accepted that camelines originated in North America and dispersed to Eurasia and Africa (e.g.

Zdansky, 1926; Teilhard de Chardin and Trassaert, 1937; Harrison, 1985; Pickford et al., 1995; Honey et al., 1998; Rybczynski et al., 2013; Wang et al., 2013; Colombero et al., 2017). While the camelines in the Old World did not radiate much as in North America and are restricted to *Paracamelus* and *Camelus* two genera only (Webb, 1965; Voorhies and Corner, 1986; Honey et al., 1998; Kostopoulos and Sen, 1999) based on the data published up to today.

Paracamelus gigas was thought to have originated from *Megatylopus gigas* of North American and migrated into Asia (Zdansky, 1926; Teilhard de Chardin and Trassaert, 1937). Their morphology was very similar to each other and Macdonald (1959) even renamed the *Megatylopus gigas* from the Middle Pliocene of Smiths Valley, Nevada, as *Paracamelus brevirostrus*. But this proposal was rejected later (Webb, 1965; Honey et al., 1998) and Voorhies and Corner (1986) suggested that the relationship of *Megatylopus* to *Paracamelus* should be re-evaluated. Made et al. (2006) considered that the dispersal of *Paracamelus* from America into the Old World seemed to have occurred in the middle of MN13, between 6.3 and 5.8 Ma, and later gave rise to the genus *Camelus*. Wang et al. (2013) pointed out that *Paracamelus* was one of a few taxa that immigrated from North America to Asia during the fauna exchange between Asia and North America in the Miocene Epoch (Arikareean through Hemphillian) in contrast to many taxa that immigrated from Asia to North America during that period. Recent revision of the camelines from Yushe Basin (Liu et al., 2023) indicated that the *P. gigas* described by Teilhard de Chardin and Trassaert (1937) could further be classified into five species and *P. gigas* was distributed only at Haiyan (Licent's Loc. 6), Qingyanping (Loc. 46) and Yimencun (Loc. 49), from Upper Mazegou Formation and Haiyan Formation, chronologically within the Late Pliocene to Early Pleistocene instead of ranging from the Late Miocene to the Early Pleistocene. The direct ancestor of *P. gigas* should therefore be from a Pliocene form rather than from the Miocene *Megatylopus*. Liu et al. (2023) considered *P. longipes* and *P. gigas* were the closest related although Geraads et al. (2021) regarded *P. longipes* as a probable variety of *P. gigas*. The new species of *Paracamelus* from Yushe Basin is the earliest record of the genus in China and it is this species that is considered as originated from North America (Liu et al., 2023).

Recent parsimony analysis on selected Old World camels (Geraads et al., 2021) with North American *Megacamelus merriami* as out group indicated that large sized *P. gigas* was a sister species of medium sized *P. alexejevi*, and they shared a common ancestor with small sized *P. alutensis.* It is understandable that most mammal taxa evolved from small sized ones to larger ones and it is acceptable the large sized *P. gigas* was derived from small sized one similar to *P. alutensis.* It implies that the earliest *Paracamelus* could be a small sized one as *P. alutensis*, but might be from a horizon in the Late Miocene or earlier and most possibly in East Asia. Based on the accessible data, the earliest appearance of *P. alutensis* is within the Pliocene (Titov, 2003). The earliest *Paracamelus* record is *Paracamelus* cf. *P. aguirrei*, a medium sized *Paracamelus*, distributed in Odessa, Eupatoria and Rostov-on-Don of East Europe and dated from 7.5 to 7.1 Ma (Vangengeim and Tesakov, 2013), earlier than that of *P. alutensis.*

Another problem is that the earliest camelini immigrated from North America should be recorded in East Asia and it remains to be proven. It is possible that the medium sized ancestor of *Paracamelus* cf. *P. aguirrei* evolved in two directions in the latest Miocene, towards larger sized ones as *P. gigas* on one hand, and to smaller sized ones as *P. alutensis* on the other. An alternative interpretation of this parsimony analysis result is that *P. alutensis* derived first from the *Paracamelus* clade, followed by *P. alexejevi*, and then *P. gigas*. This sequence is chronologically and morphometrically reasonable. It indicates that *P. gigas* might be evolved from *P. alexejevi* or a similar form. They were both found from Yushe Basin (Liu et al., 2023), and the horizon of *P. alexejevi* is lower than that of larger sized *P. gigas*, in accordance with this interpretation.

As one of only two genera of Camelini in the Old World, *Paracamelus* appeared earlier, the later appeared *Camelus* was consequently thought to have originated from the former (Boule et al., 1928; Teilhard de Chardin and Piveteau, 1930; Teilhard de Chardin and Trassaert, 1937; Webb, 1965; Pickford et al., 1995; Rybczynski et al., 2013). *P. gigas* was considered to give rise to *C. knoblochi* (Boule et al., 1928; Teilhard de Chardin and Piveteau, 1930) and then to *C. bactrianus* (Teilhard de Chardin and Trassaert, 1937). But Geraads et al. (2021) showed that *C. grattardi* from the Seraitu unit dated to c. 2.5–2.9 Ma in Ethiopia was the first derived species in *Camelus* clade; *C. sivalensis* from the Plio-Pleistocene Upper Siwaliks in South Asia was the second derived one in the clade, far away from East Africa; *C. thomasi* from the late Early Pleistocene in North Africa (Martini and Geraads, 2018) was the third derived one, far from South Asia; and extant *C. bactrianus* in East and Central Asia was the fourth derived one, far from North Africa; while *C. knoblochi* from the Middle to Late Pleistocene in Russia, Kazakhstan, Tajikistan and northern China and extant *C. dromedarius* are the crown sister species in the clade, the former appeared chronologically earlier than extant *C. bactrianus* but derived later. This result is cladistically parsimony but geographically and chronologically complicated since each specific branch of the *Camelus* clade should migrate between Africa and Eurasia from time to time at a considerable distance, while *C. knoblochi* and *C. ferus* were considered as two subspecies of *C. bactrianus* (Kostopoulos and Sen, 1999). The Early Pleistocene Dalian specimens are morphometrically close to that of the Middle and Late Pleistocene *C. knoblochi*. In addition, the geographic distribution of *P. gigas* include Tianjin (Schlosser, 1903), Mianchi (Zdansky, 1926), Nihewan (Teilhard de Chardin and Piveteau, 1930), Yushe (Teilhard de Chardin and Trassaert, 1937) of North China and Dalian of Northeast China. It had a considerable overlap with that of *C. knoblochi* such as Jilin of Northeast China (Tang et al., 2003) and Salawusu (Boule et al., 1928; Qi, 1975) and Wulanmulun (Dong et al., 2014) of Northwest China. We agree therefore the view that *P. gigas* gave rise to *C. knoblochi* as suggested by Boule et al. (1928) and Teilhard de Chardin and Piveteau (1930).

3.4 Paleoecological and chronological consideration of *P. gigas* from Jinyuan Cave

Modern equids and bovines are typical grazers, and modern camels are mostly grazers (Nowak and Paradiso, 1983). Fossil camels were also considered as grazers (Made and

Morales, 1999). *Paracamelus* were regarded as being adapted to the more arid conditions of steppe and semi-desert landscapes (Titov and Logvynenko, 2006), indicating general grazer status of these fossil camels. Although the cheek tooth crown of Dalian specimen is less hypsodont as those of bovines and equids, the dental morphology indicates that *P. gigas* from Dalian was a steppe and forest–steppe dweller fed mainly on grassy vegetation and its diet also included sprigs and leaves as *C. knoblochi* described by Titov (2008).

Layer 4 yielding the broken skull and mandibular fragment of *P. gigas* was magnetically dated to 1.1–1.8 Ma (Ge et al., 2021), with a range of 0.7 Ma. While based on pollen evidence from the deposits, the coniferous and broadleaved mixed forests developed from 1.82 to 1.76 Ma and the vegetation was dominated by forest steppe from 1.52 Ma to the Mid-Pleistocene Transition in Liaodong peninsula (Shen et al., 2021). As a steppe and forest-steppe dweller, it is more likely that *P. gigas* inhabited in Liaodong peninsula with forest steppe environment. The chronological existence of *P. gigas* from Layer 4 might further be narrowed down to 1.1–1.52 Ma, with a range of 0.42 Ma, more precisely.

4 Conclusions

The broken skull with complete right and left dentitions (DLJ168001) and the right mandibular fragment with broken m2 and complete m3 (DLJ1610-04) unearthed from Layer 4 in the Jinyuan Cave at Luotuo Hill in Dalian were identified as *Paracamelus gigas*.

Based on the fossil records and morphometric evidences, the authors infer that *P. gigas* originated from *P. alexejevi* or a similar form in the Late Pliocene in the Old World, instead of from *Megatylopus gigas* of North America and then migrated into Asia as proposed by Zdansky (1926) and Teilhard de Chardin and Trassaert (1937).

The morphometric similarities between the Early Pleistocene Dalian specimens and those of the Middle and Late Pleistocene *C. knoblochi* from North China, Russia, Kazakhstan and Tajikistan indicate that *P. gigas* gave rise to *C. knoblochi* as suggested by Boule et al. (1928) and Teilhard de Chardin and Piveteau (1930). The divergence likely happened in the late Early Pleistocene by reduction of or simplifying P3 and P4, disappearance of p3 and shortening of dentition length.

P. gigas inhabited in the forest steppe environment of Liaodong peninsula likely from 1.1 to 1.52 Ma for a period of 420 ka.

Acknowledgements The authors would like to thank Dalian Municipal Bureau for Science and Technology and Administrative Committee of Dalian Jinpu New Area for supporting the field work. They would also like to express their gratitude to Guo Yanfang for preparing the specimens. They would like to acknowledge the reviewers for their comments and suggestions to improve the manuscript. The skull DLJ168001 was photographed by Gao Wei, the palatal view of the skull of *Paracamelus gigas* housed in Uppsala Museum of Evolution was photographed by Dr. Xiong Wuyang with the permission of Uppsala Museum of Evolution.

辽宁大连骆驼山早更新世巨副驼头骨化石

董　为[1]　刘文晖[2]　白炜鹏[3]　刘思昭[4]　王　元[1]　刘金远[4]　金昌柱[1]

(1 中国科学院古脊椎动物与古人类研究所，中国科学院脊椎动物演化与人类起源重点实验室 北京 100044)

(2 中国国家博物馆环境考古研究所 北京 100006)

(3 河北师范大学历史文化学院，泥河湾考古研究院 石家庄 050024)

(4 大连自然博物馆 大连 116024)

摘要：起源于中始新世的骆驼科(Camelidae)是一支在北美的新生代期间演化非常成功的类群，具有很大的多样性。其中的一类约在中中新世期间经白令陆桥迁徙到亚洲，随后扩散到欧洲和非洲。虽然骆驼科在北美新生代期间演化辐射出很多种类，但从北美扩散到旧大陆的骆驼只有一个族(Camelini)的两个属：副驼(*Paracamelus*)和骆驼(*Camelus*)。巨副驼(*Paracamelus gigas*)是我国境内最早发现的化石骆驼，一直被认为是起源于北美的*Megatylopus*之类的大型骆驼，然后扩散到旧大陆其他地区，最后演化成诺氏驼(*Camelus knoblochi*)及双峰驼(*C. bactrianus*)。但也有学者认为骆驼属起源于非洲。最近在大连复州湾骆驼山金远洞第四纪堆积剖面的第4层中出土了一些骆驼化石，其中1件破损的头骨和带有两枚下臼齿的残破下颌骨经研究被归入巨副驼。根据对巨副驼及其他副驼种的地理及年代分布的研究，巨副驼的直接祖先应该类似于晚上新世分布在欧亚大陆的体型稍小的阿氏副驼(*P. alexejevi*)或相似类型。大连出产的巨副驼在形态及大小上与诺氏驼接近，但其齿列长度略大于诺氏驼且明显大于野生双峰驼(*C. ferus*)及单峰驼(*C. dromedarius*)。而巨副驼与诺氏驼在地理分布上的重叠范围较大，时代分布上呈先后关系，因此可以认为巨副驼是诺氏驼的直接祖先，巨副驼在中更新世晚期通过P3收缩或简化及p3消失而演化成诺氏驼。综合化石层位的古地磁测年及花粉分析结果判断，巨副驼在早更新世的1.1~1.52 Ma期间栖息在大连半岛的森林草原环境中。

关键词：大连，早更新世，洞穴堆积，骆驼，巨副驼，演化

中图法分类号：Q915.876　　**文献标识码**：A　　**文章标号**：2096–9899(2024)01–0047–22

References

Bai W P, Dong W, Liu J Y et al., 2017. New material of *Axis shansius* (Mammalia, Artiodactyla) and phylogenetic consideration of *Axis*. Quat Sci, 37(4): 821–827

Boule M, Breuil H, Licent E et al., 1928. Le Paleolithique de la Chine. Paris: Masson et cie, Editeurs. 1–138

Colombero S, Bonelli E, Pavia M et al., 2017. *Paracamelus* (Mammalia, Camelidae) remains from the late Messinian of Italy: insights into the last camels of western Europe. Hist Biol, 29(4): 509–518

Dong W, 2004. The dental morphological characters and evolution of Cervidae. Acta Anthrop Sin, 23(supp): 286–295

Dong W, Hou Y M, Yang Z M et al., 2014. Late Pleistocene mammalian fauna from Wulanmulan Paleolithic Site, Nei Mongol, China. Quatern Int, 347: 139–147

Ge J Y, Deng C L, Shao Q F et al., 2021. Magnetostratigraphic and uranium-series dating of fossiliferous cave sediments in Jinyuan Cave, Liaoning Province, northeast China. Quatern Int, 591: 5–14

Geraads D, Barr W A, Reed D et al., 2021. New remains of *Camelus grattardi* (Mammalia, Camelidae) from the Plio-Pleistocene of Ethiopia and the phylogeny of the genus. J Mammal Evol, 28: 359–370

Harington C R, 2011. Pleistocene vertebrates of the Yukon Territory. Quaternary Sci Rev, 30: 2341–2354

Harrison J A, 1985. Giant camels from the Cenozoic of North America. Smithson Contrib Paleobiol, 57: 1–29

Honey J G, Harrison J A, Prothero D R et al., 1998. Camelidae. In: Janis C M, Scott K M, Jacobs L L eds. Evolution of Tertiary Mammals of North America. Vol I: Terrestrial Carnivores, Ungulates, and Ungulatelike Mammals. New York: Cambridge University Press. 439–462

Howell F C, Fichter L S, Wolf R, 1969. Fossil camels in the Omo beds, southern Ethiopia. Nature, 223: 150–152

Hu C K, Qi T, 1978. Gongwangling Pleistocene mammalian fauna of Lantian, Shaanxi. Palaeont Sin, New Ser C, 21: 1−64

Jiangzuo Q G, Gimranov D, Liu J Y et al., 2021. A new fossil marten from Jinyuan Cave, northeastern China reveals the origin of the Holarctic marten group. Quatern Int, 591: 47–58

Jin C Z, Wang Y, Liu J Y et al., 2021. Late Cenozoic mammalian faunal evolution at the Jinyuan Cave site of Luotuo Hill, Dalian, Northeast China. Quatern Int, 577: 15–28

König H E, Liebich H-G (Translated by Chen Y X, Liu W M, Lei Z H et al.), 2009. Veterinary Anatomy of Domestic Mammals. Beijing: China Agriculture University Press. 1–808

Kostopoulos D S, Sen S, 1999. Late Pliocene (Villafranchian) mammals from Sarikol Tepe, Ankara, Turkey. Mitt Bayer Staatssamml Paläont Hist Geol, 39: 165–202

Li Y X, Ji H X, 1981. Environmental change in Peking Man's Time. Vert PalAsiat, 19(4): 337–347

Liaoning Provincial Institute of Geological Exploration, 2013. Regional Geology of Liaoning Province. Beijing: Geological Publishing House. 143–172

Likius A, Brunet M, Geraads D et al., 2003. Le plus vieux Camelidae Mammalia, Artiodactyla d'Afrique: limite Mio-Pliocène, Tchad. Bull Soc Géol Fr, 174(2): 187–193

Liu J Y, Liu J Y, Zhao H W et al., 2021. The giant short-faced hyena *Pachycrocuta brevirostris* (Mammalia, Carnivora, Hyaenidae) from Northeast Asia: a reinterpretation of subspecies differentiation and intercontinental dispersal. Quatern Int, 577: 29–51

Liu J Y, Zhang Y Q, Chi Z Q et al., 2022. A Late Pliocene *Hipparion houfenense* fauna from Yegou, Nihewan Basin and its biostratigraphic significance. Vert PalAsiat, 60(4): 278–323

Liu S Z, Wang Y, Dong W et al., 2017a. Preliminary report on the 2016's excavation at Luotuoshan Locality of Dalian, Liaoning Province. Quaternary Sci, 37(4): 908–915

Liu S Z, Dong W, Wang Y et al., 2017b. New materials of *Cervus* (*Sika*) *magnus* from Luotuoshan Locality of Dalian, Liaoning Province. Quaternary Sci, 37(4): 838–844

Liu W H, Hou S K, Zhang X X, 2023. Revision of the Late Cenozoic camelids from Yushe Basin, Shanxi, with comments on Chinese fossil camels. Quaternary Sci, 43(3): 712–751

Logvynenko V M, 2001. *Paracamelus minor* (Camelidae, Tylopoda) – a new camelid species from the Middle Pliocene of Ukraine. Vestn Zool, 35(1): 39–42

Macdonald J R, 1959. The Middle Pliocene mammalian fauna from Smiths Valley, Nevada. J Paleontol, 33(5): 872–887

Made J van der, Morales J, 1999. Family Camelidae. In: Rössner G, Hessig K eds. The Miocene Land Mammals of Europe.

München: Verlag Dr. Friedrich Pfeil. 221–224

Made J van der, Morales J, Sen S et al., 2002. The first camel from the Upper Miocene of Turkey and the dispersal of the camels into the Old World. C R Palevol, 1: 117–122

Made J van der, Morales J, Montoya P, 2006. Late Miocene turnover in the Spanish mammal record in relation to palaeoclimate and the Messinian Salinity Crisis. Palaeogeogr, Palaeoclimatol, Palaeoecol, 238: 228–246

Martini P, Geraads D, 2018. *Camelus thomasi* (Mammalia, Camelidae) from the type-locality Tighennif, Algeria. Geodiversitas, 40(5): 115–134

Matthew W D, Cook H J, 1909. A Pliocene fauna from western Nebraska. Bull Am Mus Nat Hist, 26: 361–414

Morales J, 1984. Venta del Moro: su macrofauna de mamiferos, y biostratigrafia continental del Mioceno terminal Mediterraneo. Tesis doctoral. Madrid: Editorial de la Universidad Complutense de Madrid. 1–340

Nowak R M, Paradiso J L, 1983. Walker's Mammals of the World. Baltimore: The Johns Hopkins University Press. 1–1362

Pacheco Torres V R, Enciso A A, Porras E G, 1986. The Osteology of South American Camelids. Archaeological Research Tools, Volume 3. Los Angeles: Institute of Archaeology, University of California. 1–32

Pan Y, Liu S Z, Dong W et al., 2020. New materials of *Eucladoceros* (Artiodactyla, Mammalia) from Luotuoshan Locality of Dalian, Liaoning Province. Quaternary Sci, 40(1): 275–282

Pickford M, Morales J, Soria D, 1995. Fossil camels from the Upper Miocene of Europe: implications for biogeography and faunal change. Geobios, 28(5): 641–650

Qi G Q, 1975. Quaternary mammalian fossils from Salawusu River District, Nei Mongol. Vert PalAsiat, 13(4): 239–249

Qin C, Wang Y, Liu S Z et al., 2021. First discovery of fossil *Episiphneus* (Myospalacinae, Rodentia) from Northeast China. Quatern Int, 591: 59–69

Qiu Z X, Huang W L, Guo Z H, 1987. The Chinese hipparionine fossils. Palaeont Sin, New Ser C, 25: 1–250

Qiu Z X, Qiu Z D, Deng T et al., 2013. Neogene Land Mammal Stages/Ages of China—Toward the goal to establish an Asian Land Mammal Stage/Age scheme. In: Wang X M, Flynn L J, Fortelius M eds. Fossil Mammals of Asia—Neogene Biostratigraphy and Chronology. New York: Colombia University Press. 29–90

Rybczynski N, Gosse J C, Harington C R et al., 2013. Mid-Pliocene warm-period deposits in the high arctic yield insight into camel evolution. Nat Commun, 4: 1550

Schlosser M, 1903. Die fossilen Säugethiere Chinas nebst einer Odontographie der recenten Antilopen. Abh Math Phys KL K Bayer Akad Wiss, München, 22(1): 1–220

Shen G, Gao X, Gao B et al., 2009. Age of Zhoukoudian *Homo erectus* determined with $^{26}Al/^{10}Be$ burial dating. Nature, 458: 198–200

Shen H, Zhao K L, Ge J Y et al., 2021. Early and Middle Pleistocene vegetation and its impact on faunal succession on the Liaodong Peninsula, Northeast China. Quatern Int, 591: 15–23

Shpansky A V, Aliyassova V N, Ilyina S A, 2016. The Quaternary mammals from Kozhamzhar Locality (Pavlodar Region, Kazakhstan). Am J Appl Sci, 13(2): 189–199

Stidham T A, Smith N A, Li Z H, 2021. A Pleistocene raven skull (Aves, Corvidae) from Jinyuan Cave, Liaoning Province, China. Quatern Int, 591: 80–86

Sun B, Liu S, Liu Y et al., 2021a. *Hipparion* in Luotuo Hill, Dalian, and evolution of latest *Hipparion* in China. Quatern Int,

591: 24–34

Sun B, Liu W H, Liu J Y et al., 2021b. *Equus qingyangensis* in Jinyuan Cave and its palaeozoographic significance. Quatern Int, 591: 35–46

Tang Y J, 1980. Note on a small collection of Early Pleistocene mammalian fossils from northern Hebei. Vert PalAsiat, 18(4): 314–323

Tang Y J, Zong G F, Xu Q Q, 1983. Mammalian fossils and stratigraphy of Linyi, Shanxi. Vert PalAsiat, 21(1): 77–86

Tang Z W, Liu S H, Lin Z R et al., 2003. The Late Pleistocene fauna from Dabusu of Qian'an in Jilin Province of China. Vert PalAsiat, 41(2): 137–146

Teilhard de Chardin P, Piveteau J, 1930. Les mammifères fossils de Nihowan (Chine). Ann Paléont, 19: 1–134

Teilhard de Chardin P, Trassaert M, 1937. Pliocene Camelidae, Giraffidae and Cervidae of S. E. Shansi. Palaeont Sin, New Ser C, 1: 1–56

Titov V V, 2003. *Paracamelus* from the Late Pliocene of the Black Sea Region. In: Petculescu A, Ştiucã E eds. Advances in Vertebrate Paleontology «Hen to Panta». Bucharest. 17–24

Titov V V, 2008. Habitat conditions for *Camelus knoblochi* and factors in its extinction. Quatern Int, 179: 120–125

Titov V V, Logvynenko V N, 2006. Early *Paracamelus* (Mammalia, Tylopoda) in Eastern Europe. Acta Zool Cracov, 49A: 163–178

Vangengeim E, Tesakov A S, 2013. Late Miocene mammal localities of Eastern Europe and Western Asia—toward biostratigraphic synthesis. In: Wang X M, Flynn L J, Fortelius M eds. Fossil Mammals of Asia—Neogene Biostratigraphy and Chronology. New York: Colombia University Press. 521–537

Voorhies M R, Corner R G, 1986. *Megatylopus*(?) *cochrani* (Mammalia: Camelidae): a re-evaluation. J Vert Paleont, 6(1): 65–75

Wang B Y, Wu W Y, 1979. The artiodactyla. In: IVPP ed. Vertebrate Fossils of China. Beijing: Science Press. 501–620

Wang X M, Flynn L J, Fortelius M, 2013. Introduction—toward a continental Asian biostratigraphic and geochronologic framework. In: Wang X M, Flynn L J, Fortelius M eds. Fossil Mammals of Asia—Neogene Biostratigraphy and Chronology. New York: Colombia University Press. 1–25

Webb S D, 1965. The osteology of *Camelops*. Bull Los Angeles County Mus, 1: 1–54

Yang Y H S, Li Q, Ni X J et al., 2021. Tooth micro-wear analysis reveals that persistence of beaver *Trogontherium cuvieri* (Rodentia, Mammalia) in Northeast China relied on its plastic ecological niche in Pleistocene. Quatern Int, 591: 70–79

Young C C, 1932. On the Artiodactyla from the *Sinanthropus* Site at Chouk'outien. Palaeont Sin, Ser C, 8: 1–158

Zazula G D, Macphee R, Hall E et al., 2016. Osteological assessment of Pleistocene *Camelops hesternus* (Camelidae, Camelinae, Camelini) from Alaska and Yukon. Am Mus Novit, 3866: 1–45

Zdansky O, 1926. *Paracamelus gigas* Schlosser. Palaeont Sin, Ser C, 2(4): 1–44

Zhang Y X, Sun D H, An Z S et al., 1999. Mammalian fossils from Late Pliocene (lower MN16) of Lingtai, Gansu Province. Vert PalAsiat, 37(3): 190–199

Zhao S S, Pei J X, Guo S L et al., 1985. Study of chronology of Peking Man Site. In: Wu R K, Ren M E, Zhu X M et al. eds. Multi-disciplinary Study of the Peking Man Site at Zhoukoudian. Beijing: Science Press. 239–240